Title

Dynamic, Cell-Type-Specific Roles for GABAergic Interneurons in a Mouse Model of Optogenetically Inducible Seizures

Journal

Neuron, 93(2)

ISSN

0896-6273

Authors

Khoshkhoo, Sattar
Vogt, Daniel
Sohal, Vikaas S

Publication Date

2017

DOI

10.1016/j.neuron.2016.11.043

Peer reviewed

HHS Public Access

Author manuscript

Neuron. Author manuscript; available in PMC 2018 January 18.

Published in final edited form as:

Neuron. 2017 January 18; 93(2): 291–298. doi:10.1016/j.neuron.2016.11.043.

Dynamic, cell type-specific roles for GABAergic interneurons in a mouse model of optogenetically inducible seizures

Sattar Khoshkhoo[1,2,3,4], **Daniel Vogt**[1,2,3], and **Vikaas S. Sohal**[1,2,3,4,*]

[1]Department of Psychiatry University of California, San Francisco San Francisco, CA 94143-0444

[2]Weil Institute for Neurosciences University of California, San Francisco San Francisco, CA 94143-0444

[3]Kavli Institute for Fundamental Neuroscience University of California, San Francisco San Francisco, CA 94143-0444

[4]Sloan Swartz Center for Theoretical Neurobiology University of California, San Francisco San Francisco, CA 94143-0444

SUMMARY

GABAergic interneurons play critical roles in seizures, but it remains unknown whether these vary across interneuron subtypes or evolve during a seizure. This uncertainty stems from the unpredictable timing of seizures in most models, which limits neuronal imaging or manipulations around the seizure onset. Here, we describe a mouse model for optogenetic seizure induction. Combining this with calcium imaging, we find that seizure onset rapidly recruits parvalbumin (PV), somatostatin (SOM), and vasoactive intestinal peptitde (VIP)-expressing interneurons, whereas excitatory neurons are recruited several seconds later. Optogenetically inhibiting VIP interneurons consistently increased seizure threshold and reduced seizure duration. Inhibiting PV+ and SOM+ interneurons had mixed effects on seizure initiation, but consistently reduced seizure duration. Thus, while their roles may evolve during seizures, PV+ and SOM+ interneurons ultimately help maintain ongoing seizures. These results show how an optogenetically-induced seizure model can be leveraged to pinpoint a new target for seizure control: VIP interneurons.

INTRODUCTION

Epilepsy has many genetic (Mantegazza et al., 2010) and acquired (Shorvon, 2011) causes. For almost all of these, GABAergic interneurons play critical roles in regulating the activity of cortical microcircuits implicated in seizures and epilepsy (Paz and Huguenard, 2015). Nevertheless, the exact role of GABAergic interneurons in seizure initiation, propagation, maintenance, and termination is still debated. Studies in mice have shown that enhancing

*To whom correspondence should be addressed at vikaas.sohal@ucsf.edu.

AUTHOR CONTRIBUTIONS SK performed the experiments. DV performed immunohistochemistry. SK and VS designed the experiments and wrote the paper.

interneuron output, by either transplanting medial ganglionic eminence (MGE)-derived interneuron precursors (Hunt et al., 2013) or optogenetically activating parvalbumin-expressing (PV+) interneurons (Krook-Magnuson et al., 2013), can decrease seizure frequency or promote seizure termination. Whereas these findings support a role for interneurons in suppressing seizures, other studies have proposed that interneurons could contribute to excessive neuronal synchronization in ways that promote seizures (Alvarado-Rojas et al., 2013; Ellender et al., 2014). One mechanism through which interneurons may contribute to seizures is by eliciting depolarizing GABAergic currents (Alger and Nicoll, 1979; Andersen et al., 1980; Perreault and Avoli, 1992). Thus, whereas it is clear that under certain conditions, increasing interneuron output suppresses seizures, it remains unclear whether this is always the case, or whether interneurons can at times act to promote seizures.

Further complicating matters, cortical GABAergic interneurons comprise numerous heterogeneous subtypes, and the roles of many of these remain unknown. Unlike MGE-derived PV+ and somatostatin-expressing (SOM+) interneurons, whose roles in seizures have frequently been studied (Paz and Huguenard, 2015), little is known about the contribution of a distinct population of interneurons which express vasoactive intestinal peptide (VIP). VIP+ interneurons are believed to synapse primarily onto other GABAergic interneurons and play a disinhibitory role in cortical circuits (Lee et al., 2013; Pi et al., 2013). Three observations suggest a possible role for VIP+ interneurons in seizures: VIP levels are increased in the CSF of children with chronic epilepsy (Ko et al., 1991); levels of VIP receptor binding are increased in post-mortem tissue from individuals with temporal lobe epilepsy (de Lanerolle et al., 1995); and VIP+ interneuron firing increases as spike and wave discharges develop in tubocurarine-treated rat cortical slices (Hall et al., 2015). Nevertheless, the significance of these findings remains unknown.

Some of the uncertainty around the role of interneurons stems from the fact that *in vivo*, systems-level investigations of seizures have been challenging. This is largely because most *in vivo* models of chronic epilepsy develop spontaneous seizures (Raol and Brooks-Kayal, 2012). This lack of temporal control over seizure onset limits the use of advanced imaging and cellular manipulation techniques, such as Ca^{2+} imaging and optogenetics.

Here, we address some of these issues by first developing an *in vivo* optogenetically-inducible mouse model of ictogenesis that captures key features of clinically observed seizures. We then use this model together with cell type-specific bulk Ca^{2+} imaging to measure the activity patterns of specific classes of interneurons and excitatory neurons during seizures. Finally, we use targeted optogenetic inhibition in this model to show that VIP+ and MGE-derived (PV+ and SOM+) interneurons play different roles in seizures.

RESULTS

Optogenetic seizure induction

To induce seizures optogenetically, we used a novel protocol combining multiple stimulation frequencies and light intensities to focally activate ChR2 in the mouse primary motor cortex (Experimental Procedures; Figure 1A). Significantly more seizures occurred following high (20–40Hz) vs. low (5–10Hz) frequency stimulation ($p<0.001$ by ANOVA; $p<0.05$ for 20 and

40Hz vs. 5 and 10Hz stimulation by Tukey-Kramer (TK) multiple comparisons test; Figure S1I). On average 10–15 optical stimuli were required to induce the first seizure, however, this varied slightly depending on mouse genotype ($p<10^{-6}$ by ANOVA; n=4–6 mice for each genotype; Figure S1E). After the first seizure, the probability of seizure induction with each subsequent stimulus was consistently >70%. We did not observe seizures in the absence of a stimulus, even after optogenetic seizure induction. Interestingly, the onset of electrographic and behavioral seizure activity was delayed by 1-2 minutes following the delivery of each stimulus (Figure S1A). The number of stimuli required to elicit the initial seizure was specific to each mouse and did not change significantly across three days of experimentation (p=0.27 by ANOVA; Figure S1F).

Based on electrographic criteria alone (Experimental Procedures), the majority of seizures (79±5%) were primarily generalized at onset, i.e., no initial seizure focus could be identified (Figure S1J). The remaining seizures were mainly focal with secondary generalization (18±2%); a select few were focal (3±3%) (Figure S1J). Interestingly, when an electrographic focus could be identified, it was more often (65±15%) *contralateral* to the site of ChR2 stimulation. Optogenetically-induced seizures typically began as bilateral periodic discharges that first evolved into bursts, then into high frequency, high amplitude spikes that terminated spontaneously (Figure S1B–D). The majority of seizures in all genotypes ranged from stage 3 (unilateral and bilateral limb clonus) to stage 5 (generalized clonic seizures) on a modified Racine scale (Experimental Procedures; Figure S1K). The average seizure duration was 64±6 seconds and there were no significant differences in duration across genotypes (p=0.89 via ANOVA; n=19–47 seizures for each genotype; Figure S1G), or the three days of experimentation (p=0.35 by ANOVA; n=31, 43, and 39 seizures on days 1, 2, and 3; Figure S1H).

Cell type-specific bulk calcium imaging

We combined our optogenetic seizure model with fiber photometry (Cui et al., 2014; Gunaydin et al., 2014) to perform cell type-specific bulk Ca^{2+} imaging during seizures (Experimental Procedures; Figure 1A). We used PV-Cre, SOM-Cre, and VIP-Cre mice to label the major classes of cortical GABAergic interneurons, and Emx1-Cre mice to target the majority of excitatory neurons in neocortex. During each recording session, we optogenetically induced seizures, as described above, while simultaneously recording electrical signals via EEG and Ca^{2+} signals via fiber photometry.

Seizures produced large Ca^{2+} signals in all studied cell types – normalized signals (ΔF/F) were ~1–3 fold higher than baseline (Figure 1B, Figure S2A–D). Ca^{2+} signals were highly correlated with individual low-frequency electrographic discharges in the ipsilateral EEG recording (Figure 1C). Individual Ca2+ transients associated with higher frequency EEG spikes (>5 Hz) could not be resolved, presumably due to the kinetics of GCaMP6f (Figure 1D).

Interneurons and excitatory neurons exhibit unique patterns of activity during seizures

To compare the activity of different cell types around seizure initiation, we identified the time of electrographic seizure onset, then aligned and averaged all EEG and photometry

recordings (Experimental Procedures). The averaged traces show that in PV+, SOM+, and VIP+ interneurons, Ca^{2+} signals increased sharply upon seizure onset (Figure 2Ai, Bi, Ci). In contrast, in Emx1+ neurons, the rise in Ca^{2+} signals was delayed by ~10s following seizure onset (Figure 2Di). To quantify this, we compared Ca^{2+} signals 5s before vs. 5s after seizure onset for each cell type (Figure 2Aii–Dii). Ca^{2+} signals after seizure onset were significantly greater than 5s before seizure onset for all three interneuron subtypes, but not for EMX1+ neurons ($p<0.001$–0.01 for PV-Cre, SOM-Cre, and VIP-Cre; $p=0.66$ for Emx1-Cre by two-tail paired t-test; n=15–34 seizures for each genotype). Importantly, Ca^{2+} signals in EMX1+ neurons were not weaker than those in interneurons (Figure 2Di). Also, the averaged aligned EEG traces demonstrated a similar, sharp rise in normalized power at the time of seizure onset for all Cre lines (Figure 2Ai–Di). Thus these differences in Ca^{2+} signals at the time of seizure onset are not simply artifacts of differences in the seizure dynamics between EMX1-Cre mice and other genotypes.

To compare the activity of different cell types during seizure maintenance and around seizure termination, we created the compressed time plots shown in Figures 2Aiii–Diii. Each compressed time plot was aligned to both seizure initiation and seizure termination, making it possible to compare mean EEG and photometry signals from seizures with different durations. Based on these plots, Ca^{2+} signals in PV+ and SOM+ neurons increase after seizure onset, then remain maximal until seizure termination (Figure 2Aiii, Biii). By contrast, Ca^{2+} signals in VIP+ and Emx1+ neurons appear to peak mid-seizure, then decline before seizure termination (Figure 2Ciii, Diii). Again, to quantify these observations, we compared Ca^{2+} signals for each genotype at the following timepoints: first data point (in compressed time) after seizure onset, at the peak of the trace, first data point (compressed time) prior to seizure termination, and 1s after seizure termination (Fig. 2Aiv–Div). For every cell type, the peak Ca^{2+} signal during the seizure was significantly greater than at seizure onset ($p<10^{-6}$–0.05; n=11–23 seizures for each genotype), and Ca^{2+} signals were greater at the electrographic seizure termination than the post-termination timepoint ($p<10^{-6}$–0.001). However, for VIP+ and Emx1+ neurons, the peak Ca^{2+} signal was also significantly greater than the Ca^{2+} signal at seizure termination (VIP: $p<10^{-4}$, Emx: $p<0.05$), indicating that Ca^{2+} signals in VIP+ and Emx1+ neurons decrease well before seizure termination. By contrast, for PV+ and SOM+ neurons, Ca^{2+} signals at termination were not significantly different from their peak values.

Notably, all three interneuron Cre lines had high specificity (PV-Cre: 95 ± 1%, SOM-Cre: 84 ± 2%, VIP-Cre: 77 ± 1%; Figure S2E–G) and reasonable sensitivity (PV-Cre: 65 ± 4%, SOM-Cre: 49 ± 9%, VIP-Cre: 63 ± 4%; Figure S2E–G) for GCaMP expression. No GABAergic interneurons were labeled with GCaMP in Emx1-Cre mice (Figure S2H).

To investigate how specific cell populations contribute to electrographic signals at seizure onset, we attempted to disrupt local field potentials (LFPs) associated with seizures using cell type-specific optogenetic inhibition. To our surprise, neither specific inhibition of PV+, SOM+, or Emx1+ neurons, nor inhibition of *all* neurons using a synapsin promoter attenuated electrographic seizure activity (n=2–6 mice for each case; Figure S3H–K). Importantly, in Emx1-Cre mice, LFPs at the cannula implantation site increased immediately upon seizure onset (n=2 mice and 5 seizures; Figure S2I). This reaffirms that the delayed

increase of Ca2+ signals in excitatory cells after seizure onset cannot be attributed to the absence of local electrographic seizure activity, but rather reflects the specific absence of neuronal activity in excitatory neurons.

Using optogenetic inhibition to test causal roles for interneurons in seizures

We used eArch3.0 to selectively inhibit either VIP+ interneurons, DlxI12b-labeled interneurons, PV+ interneurons, or SOM+ interneurons during optogenetically-induced seizures (Figure 3A; Figure S3A–C,L). DlxI12b labels 80–90% of PV+ and SOM+ interneurons and many fewer calretinin (CR)+ interneurons, a small subset of which are VIP + (Potter et al., 2009). First, we looked at the effects of interneuron inhibition during the pre-ictal phase. Inhibiting VIP+ interneurons *contralateral* (but not ipsilateral) to the stimulation site significantly increased seizure threshold, shown by a rightward shift of the cumulative probability distribution for seizure probability vs. number of stimuli ($p<10^{-8}$ between baseline and –contra via TK multiple comparisons test; n=5 mice; Figure 3C). Similarly, the number of optogenetic stimuli required to induce the first seizure increased with inhibition of VIP+ interneurons contralateral to the stimulation site ($p<0.05$ via two-tail t-test; n=5 mice; Figure 3D). Importantly, there was no significant change in seizure threshold in control mice expressing eYFP in VIP+ interneurons across three days of experimentation (ipsilateral: p=0.82, contralateral: p=0.16 by two-tail t-test; n=4 mice; Figure 3D).

In contrast, inhibiting DlxI12b+ interneurons, both ipsilateral and contralateral to the stimulation site, *decreased* seizure threshold (ipsilateral: $p<0.01$, contralateral: $p<0.001$ via TK multiple comparisons test; n=7 mice; Figure 3B). Both ipsilateral and contralateral inhibition of DlxI12b+ interneurons decreased the number of stimuli needed to elicit the first seizure (ipsilateral: $p<0.05$; contralateral: $p<0.01$ by two-tail t-test; n=7 mice; Figure 3D).

Repeating this experiments using more specific PV-Cre and SOM-Cre mouse lines yielded more complex results. Ipsilateral and contralateral inhibition of SOM+ interneurons alone had no effect on seizure probability (p=0.75–0.98 by TK multiple comparisons test; n=4 mice; Figure S3E) or seizure threshold (ipsilateral: p=0.55–0.63 by two-tail t-test; n=4 mice; Figure S3F). Contralateral inhibition of PV+ interneurons actually decreased seizure probability ($p<0.05$ between baseline and –contra via TK multiple comparisons test; n=6 mice; Figure S3D) and increased seizure threshold ($p<0.05$ by two-tail t-test; Figure S3F). Ipsilateral PV+ inhibition had negligible effects (Figure S3D, S3F).

We also analyzed the effects of interneuron inhibition on seizure maintenance and termination. Consistent with the antiseizure effects of inhibiting VIP+ interneurons on seizure initiation, we found that inhibiting VIP+ interneurons contralateral to the stimulation site shortened seizure duration ($p<0.01$ by two-tail t-test; n=5 mice; Figure 3E). Surprisingly, in stark contrast to the pro-seizure effects of inhibiting DlxI12b+ interneurons during seizure initiation, inhibition of DlxI12b+ interneurons either ipsi- or contralateral to the stimulation site significantly *reduced* seizure length (ipsilateral: $p<10^{-6}$, contralateral $p<0.001$ by two-tail t-test; n=7 mice; Figure 3E).

Consistent with the reduced seizure duration observed after inhibiting DlxI12b+ interneurons, both ipsilateral and contralateral inhibition of SOM+ interneurons alone

reduced seizure duration (ipsilateral: $p<10^{-5}$, contralateral: $p<0.05$ by two-tail t-test; n=4 mice; Figure S3G). Contralateral inhibition of PV+ interneurons also reduced seizure duration ($p<0.01$; n=6 mice; Figure S3G); ipsilateral inhibition of PV+ interneurons elicited a borderline-significant reduction in seizure duration (ipsilateral: p=0.06; n=6 mice; Figure S3G). Again, there was no significant change in seizure duration in control mice expressing eYFP in VIP+ interneurons across three days of experimentation (n=4 mice; Figure 3E).

Post-ictal EEG depression is associated with cortical spreading depression (CSD)-like events

52±7% of seizures were associated with large, prolonged (~1-2 min) increases in Ca^{2+} signals, almost always after seizure termination, which resembled cortical spreading depression (CSD) (Figure 4A–B). During these events, the EEG electrode closest to the photometry site typically exhibited a broadband decrease in power (Figure 4C). The reduction in EEG power was localized–EEG power was significantly higher on the contralateral side ($p<0.001$ for all genotypes/cell types, n=9–29 events for each genotype; Figure S4B–E). These characteristics, i.e., a localized reduction in electrical activity that coincides with a strong increase in Ca^{2+} signals and lasts ~1-2 min, are consistent with post-ictal depression and also match those recently reported by a study of CSD that also used GCaMP imaging (Enger et al., 2015). CSD-like events did not happen in the absence of seizures and almost always followed seizure termination (Figure 4D). However, some CSD-like events could precede seizure termination. Interestingly, these resulted in a dramatic reduction in the power of electrographic seizure activity (Figure S4A).

CSD-like events were similar in photometry measurements from different cell types. There were no difference in event length (p=0.13 via ANOVA; Figure 4E) or onset time relative to seizure termination (p=0.99 by ANOVA; Figure 4D). The time from event onset to peak was significantly longer in Emx1+ neurons compared to interneurons ($p<0.001$ for PV-Cre vs. Emx-1-Cre, $p<0.01$ for SOM-Cre vs. Emx1-Cre, $p<0.001$ for VIP-Cre vs. Emx1-Cre via TK multiple comparisons test; Figure 4F).

DISCUSSION

We developed an optogenetic model for inducing seizures in awake, freely moving mice. Using this model, we performed cell type-specific Ca^{2+} imaging and optogenetic inhibition to elucidate roles of interneurons in various stages of seizures. Seizures recruit interneurons within <1s of seizure onset, whereas the recruitment of excitatory neurons follows after a delay of ~10s. Furthermore, Ca^{2+} signals in PV+ and SOM+ interneurons remain maximal until seizure termination, whereas Ca^{2+} signals in VIP+ interneurons and excitatory neurons begin to decrease well before the end of the electrographic seizure. During the pre-ictal period, inhibiting PV+ and SOM+ interneurons could either increase or decrease the seizure threshold, depending on whether they were inhibited selectively (using PV− and SOM− Cre mice), or simultaneously (using DlxI12b-Cre mice). However, during the ictal stage, inhibiting PV+ and/or SOM+ interneurons consistently prolonged seizures. By contrast, inhibiting VIP+ interneurons increased the threshold for seizure initiation and decreased

seizure length, suggesting that these interneurons are consistently disinhibitory and pro-seizure.

An optogenetic mouse model for seizures

The optogenetic model for seizure induction described here may complement other models of seizures. In contrast to traditional electrical kindling models (Raol and Brooks-Kayal, 2012), optogenetic seizure induction occurs relatively rapidly and the threshold for seizure induction returns to baseline each day. This makes it possible to design experiments that span multiple days in order to compare the effects of different manipulations (e.g., the optogenetic inhibition of interneurons used here). Moreover, seizures occur at a stereotyped delay (~1-2 min) following the stimulus, creating a window of opportunity for imaging and/or cellular manipulation prior to seizure initiation.

Interestingly, optogenetically-evoked seizures were often followed by events that had features consistent with both post-ictal EEG depression and cortical spreading depression. Notably, previous studies have implicated Ca^{2+} influx in post-ictal hyperpolarization (Lopantsev and Taranenko, 1990).

The function of PV+ and SOM+ interneurons during seizure initiation

We found that interneurons are rapidly recruited at seizure onset. This finding is consistent with previous work showing pre-ictal increases in the synchrony (Grasse et al., 2013) and firing rate (Toyoda et al., 2015) of interneurons in pilocarpine-treated rats and a patient with focal epilepsy (Truccolo et al., 2011). Notably, the recruitment of interneurons precedes that of excitatory neurons by several seconds. There are two possible explanations for this observation. One is that the rapid recruitment of interneurons results, at least transiently, in reduced local excitability (Bragin et al., 2005) and decreased principal cell firing (Bower and Buckmaster, 2008). Another possibility is that interneurons contribute to seizure initiation. We found evidence for both scenarios. Silencing a large population of DlxI12b-labeled PV+ and SOM+ interneurons significantly reduced seizure threshold, consistent with the idea that a global reduction in inhibition makes seizures more likely. However when we selectively inhibited smaller populations of PV+ and SOM+ interneurons, we observed either no effect on seizure threshold (in SOM-Cre mice), or an increase in seizure threshold (in PV-Cre mice).

Why did we observe different effects on seizure threshold – no change, an increase, or a decrease – in PV-Cre, SOM-Cre, and DlxI12b-Cre mice, respectively? Although the use of PV-Cre and SOM-Cre mice to selectively label PV+ or SOM+ interneurons has excellent specificity, the sensitivity is more modest (Figure S2E–F). This is a particular concern for PV+ and SOM+ interneurons given their high degree of interconnectivity. Because of this, inhibiting only a subset of PV or SOM interneurons might actually *disinhibit* many remaining interneurons. By contrast, DlxI12b-Cre mice label the majority of both cortical PV+ and SOM+ interneurons (Potter et al., 2009), making them less susceptible to this potential issue. With this in mind, the discordant effects we observed on seizure threshold may reflect differences in the ability of various manipulations to disrupt overall levels of circuit inhibition. Alternatively, differences in genetic background may explain why

inhibiting interneurons has different effects on seizure threshold in PV-Cre, SOM-Cre, and DlxI12b-Cre mice.

The function of PV+ and SOM+ interneurons during seizure maintenance

We also examined whether interneurons play the same or different roles during seizure maintenance and termination compared to seizure initiation. PV+ and SOM+ interneurons maintain high Ca^{2+} signals until seizure termination, suggesting strong interneuron recruitment during seizures. Our observations that inhibiting PV+ and/or SOM+ interneurons, either selectively or at the same time (using DlxI12b-Cre mice) consistently reduces seizure duration suggests that these interneurons play an important role in seizure maintenance during the ictal stage. PV+ interneurons may contribute to this process (Ellender et al., 2014) by recruiting depolarizing GABAergic synaptic potentials (Alger and Nicoll, 1979; Andersen et al., 1980; Perreault and Avoli, 1992). It is possible that intense ongoing synaptic activity over the course of a seizure drives intracellular chloride accumulation by causing a shift in the reversal potential (Arellano et al., 2004; Staley et al., 1995).

VIP+ interneurons maintain a disinhibitory role throughout the seizure

Previous studies have shown that mice with reduced numbers of VIP+ interneurons are `seizure resistant' (Lodato et al., 2011) and bath application of a VIP receptor antagonist can decrease the incidence of acute tubocurarine-induced spike and wake discharges in rat cortical slices (Hall et al., 2015). These observations are in agreement with the hypothesis that VIP+ interneurons have a predominately disinhibitory role in cortical circuits (Lee et al., 2013; Pi et al., 2013). Consistent with this, we found that preictal inhibition of VIP+ interneurons significantly increased the threshold for optogenetic seizure induction. Additionally, ictal inhibition of VIP+ interneurons decreased seizure length. These findings demonstrate that inhibition of VIP+ interneurons has a consistent anti-seizure effect (Figure 3F). This effect should be tested in models of chronic epilepsy and could be exploited for the development of new antiepileptic treatments.

Limitations and future directions

For seizure induction, we expressed ChR2 under control of the commonly used CaMKIIα1.3 promoter, which is only 82% specific for excitatory neurons (Scheyltjens et al., 2015). Thus, it would be informative to explore how optogenetic stimulation of specific neuronal subpopulations contributes to seizure induction. Our study also relies on photometry, which enables cell type-specific activity measurements in freely moving mice, but is limited by the temporal resolution of existing GCaMP sensors, and lacks spatial resolution. Other imaging methods, e.g., two-photon microscopy or microendoscopy could add additional details about interactions between individual neurons.

Additionally, our findings rely on the assumption that intracellular Ca^{2+} reliably indicates neuronal activity. While the bevy of recent studies using similar approaches underscore the presumption that that this is generally valid, GCaMP imaging cannot distinguish neuronal firing from other possible drivers of Ca^{2+} influx. Nevertheless, an important observation is that the magnitudes of signals, e.g., peak amplitudes of ΔF/F, were broadly similar in

excitatory and inhibitory neurons, suggesting that differences in these signals do not simply reflect cell type differences in the sensitivity of GCaMP sensors.

Puzzlingly, we were unable to identify the source of LFPs using cell type specific optogenetic inhibition. A possible explanation is that the spatial extent of optogenentic inhibition is relatively small. As such, cell type specific inhibitory tools with broader spatial coverage, e.g., DREADDs, would be interesting to use in the future.

As discussed above, PV+ and/or SOM+ interneurons may help maintain seizures by recruiting depolarizing GABAergic currents following the intracellular accumulation of chloride. Future studies could evaluate this directly using the genetically encoded chloride indicator, Clomeleon (Kuner and Augustine, 2000), together with photometry (Wells et al., 2016) to measure intracellular chloride changes during seizures.

Finally, although our optogenetic model for seizure induction allowed us to overcome certain experimental challenges, it does not reproduce the spontaneous seizures that occur in chronic epilepsy. Thus, optogenetic seizure induction is best thought of as an adjunctive tool, which complements genetic and pharmacologic models of epilepsy. Future studies should both revisit our findings using well-validated models of epilepsy, and validate the effects of anticonvulsant drugs in optogenetic seizure model.

EXPERIMENTAL PROCEDURES

Full Experimental Procedures are in the Supplemental Information.

Supplementary Material

Refer to Web version on PubMed Central for supplementary material.

ACKNOWLEDGEMENTS

We thank Daniel Lowenstein and Jeanne Paz for helpful comments on the manuscript, K. Cho, M. Cunniff, J. Iafrati, and A. Lee for assistance with slice electrophysiology, and R. Mayeda for scoring seizures. SK was supported by the HHMI Medical Research Fellows Program and Citizens United for Research in Epilepsy (CURE). VS was supported by NIMH (U01MH105948) and the NIH Office of the Director (DP2MH100011).

REFERENCES

Alger BE, Nicoll RA. GABA-mediated biphasic inhibitory responses in hippocampus. Nature. 1979; 281:315–317. [PubMed: 551280]

Alvarado-Rojas C, Lehongre K, Bagdasaryan J, Bragin A, Staba R, Engel J, Navarro V, Le Van Quyen M. Single-unit activities during epileptic discharges in the human hippocampal formation. Front. Comput. Neurosci. 2013; 7:140. [PubMed: 24151464]

Andersen P, Dingledine R, Gjerstad L, Langmoen IA, Laursen AM. Two different responses of hippocampal pyramidal cells to application of gamma-amino butyric acid. J. Physiol. 1980; 305:279–296. [PubMed: 7441554]

Arellano JI, Muñoz A, Ballesteros-Yáñez I, Sola RG, DeFelipe J. Histopathology and reorganization of chandelier cells in the human epileptic sclerotic hippocampus. Brain J. Neurol. 2004; 127:45–64.

Bower MR, Buckmaster PS. Changes in granule cell firing rates precede locally recorded spontaneous seizures by minutes in an animal model of temporal lobe epilepsy. J. Neurophysiol. 2008; 99:2431–2442. [PubMed: 18322007]

Bragin A, Azizyan A, Almajano J, Wilson CL, Engel J. Analysis of chronic seizure onsets after intrahippocampal kainic acid injection in freely moving rats. Epilepsia. 2005; 46:1592–1598. [PubMed: 16190929]

Cui G, Jun SB, Jin X, Luo G, Pham MD, Lovinger DM, Vogel SS, Costa RM. Deep brain optical measurements of cell type-specific neural activity in behaving mice. Nat. Protoc. 2014; 9:1213–1228. [PubMed: 24784819]

Ellender TJ, Raimondo JV, Irkle A, Lamsa KP, Akerman CJ. Excitatory effects of parvalbumin-expressing interneurons maintain hippocampal epileptiform activity via synchronous afterdischarges. J. Neurosci. Off. J. Soc. Neurosci. 2014; 34:15208–15222.

Enger R, Tang W, Vindedal GF, Jensen V, Helm PJ, Sprengel R, Looger LL, Nagelhus EA. Dynamics of Ionic Shifts in Cortical Spreading Depression. Cereb. Cortex. 2015; 25:4469–4476. [PubMed: 25840424]

Grasse DW, Karunakaran S, Moxon KA. Neuronal synchrony and the transition to spontaneous seizures. Exp. Neurol. 2013; 248:72–84. [PubMed: 23707218]

Gunaydin LA, Grosenick L, Finkelstein JC, Kauvar IV, Fenno LE, Adhikari A, Lammel S, Mirzabekov JJ, Airan RD, Zalocusky KA, et al. Natural neural projection dynamics underlying social behavior. Cell. 2014; 157:1535–1551. [PubMed: 24949967]

Hall S, Hunt M, Simon A, Cunnington LG, Carracedo LM, Schofield IS, Forsyth R, Traub RD, Whittington MA. Unbalanced Peptidergic Inhibition in Superficial Neocortex Underlies Spike and Wave Seizure Activity. J. Neurosci. Off. J. Soc. Neurosci. 2015; 35:9302–9314.

Hunt RF, Girskis KM, Rubenstein JL, Alvarez-Buylla A, Baraban SC. GABA progenitors grafted into the adult epileptic brain control seizures and abnormal behavior. Nat. Neurosci. 2013; 16:692–697. [PubMed: 23644485]

Ko FJ, Chiang CH, Liu WJ, Chiang W. Somatostatin, substance P, prolactin and vasoactive intestinal peptide levels in serum and cerebrospinal fluid of children with seizure disorders. Gaoxiong Yi Xue Ke Xue Za Zhi. 1991; 7:391–397. [PubMed: 1714968]

Krook-Magnuson E, Armstrong C, Oijala M, Soltesz I. On-demand optogenetic control of spontaneous seizures in temporal lobe epilepsy. Nat. Commun. 2013; 4:1376. [PubMed: 23340416]

Kuner T, Augustine GJ. A genetically encoded ratiometric indicator for chloride: capturing chloride transients in cultured hippocampal neurons. Neuron. 2000; 27:447–459. [PubMed: 11055428]

de Lanerolle NC, Gunel M, Sundaresan S, Shen MY, Brines ML, Spencer DD. Vasoactive intestinal polypeptide and its receptor changes in human temporal lobe epilepsy. Brain Res. 1995; 686:182–193. [PubMed: 7583284]

Lee S, Kruglikov I, Huang ZJ, Fishell G, Rudy B. A disinhibitory circuit mediates motor integration in the somatosensory cortex. Nat. Neurosci. 2013; 16:1662–1670. [PubMed: 24097044]

Lodato S, Tomassy GS, Leonibus ED, Uzcategui YG, Andolfi G, Armentano M, Touzot A, Gaztelu JM, Arlotta P, Prida L.M. de la, et al. Loss of COUP-TFI Alters the Balance between Caudal Ganglionic Eminence- and Medial Ganglionic Eminence-Derived Cortical Interneurons and Results in Resistance to Epilepsy. J. Neurosci. 2011; 31:4650–4662. [PubMed: 21430164]

Lopantsev VE, Taranenko VD. Paroxysmal afterpotentials and role of calcium-dependent potassium conductivity in neuronal activity of strychninized neocortex. Neuroscience. 1990; 38:137–143. [PubMed: 2123972]

Mantegazza M, Rusconi R, Scalmani P, Avanzini G, Franceschetti S. Epileptogenic ion channel mutations: From bedside to bench and, hopefully, back again. Epilepsy Res. 2010; 92:1–29. [PubMed: 20828990]

Paz JT, Huguenard JR. Microcircuits and their interactions in epilepsy: is the focus out of focus? Nat. Neurosci. 2015; 18:351–359. [PubMed: 25710837]

Perreault P, Avoli M. 4-aminopyridine-induced epileptiform activity and a GABA-mediated long-lasting depolarization in the rat hippocampus. J. Neurosci. Off. J. Soc. Neurosci. 1992; 12:104–115.

Pi H-J, Hangya B, Kvitsiani D, Sanders JI, Huang ZJ, Kepecs A. Cortical interneurons that specialize in disinhibitory control. Nature. 2013; 503:521–524. [PubMed: 24097352]

Potter GB, Petryniak MA, Shevchenko E, McKinsey GL, Ekker M, Rubenstein JLR. Generation of Cre-transgenic mice using Dlx1/Dlx2 enhancers and their characterization in GABAergic interneurons. Mol. Cell. Neurosci. 2009; 40:167–186. [PubMed: 19026749]

Raol, YH., Brooks-Kayal, AR. Chapter 1 - Experimental Models of Seizures and Epilepsies. In: Conn, PM., editor. Progress in Molecular Biology and Translational Science. Academic Press; 2012. p. 57-82.

Scheyltjens I, Laramée M-E, Van den Haute C, Gijsbers R, Debyser Z, Baekelandt V, Vreysen S, Arckens L. Evaluation of the expression pattern of rAAV2/1, 2/5, 2/7, 2/8, and 2/9 serotypes with different promoters in the mouse visual cortex. J. Comp. Neurol. 2015; 523:2019–2042. [PubMed: 26012540]

Shorvon SD. The etiologic classification of epilepsy. Epilepsia. 2011; 52:1052–1057. [PubMed: 21449936]

Staley KJ, Soldo BL, Proctor WR. Ionic mechanisms of neuronal excitation by inhibitory GABAA receptors. Science. 1995; 269:977–981. [PubMed: 7638623]

Toyoda I, Fujita S, Thamattoor AK, Buckmaster PS. Unit Activity of Hippocampal Interneurons before Spontaneous Seizures in an Animal Model of Temporal Lobe Epilepsy. J. Neurosci. Off. J. Soc. Neurosci. 2015; 35:6600–6618.

Truccolo W, Donoghue JA, Hochberg LR, Eskandar EN, Madsen JR, Anderson WS, Brown EN, Halgren E, Cash SS. Single-neuron dynamics in human focal epilepsy. Nat. Neurosci. 2011; 14:635–641. [PubMed: 21441925]

Wells MF, Wimmer RD, Schmitt LI, Feng G, Halassa MM. Thalamic reticular impairment underlies attention deficit in Ptchd1(Y/−) mice. Nature. 2016; 532:58–63. [PubMed: 27007844]

HIGHLIGHTS

- We describe a novel protocol for reliable optogenetic induction of seizures
- Seizure-related interneuron activity precedes that of excitatory neurons
- Inhibiting VIP+ interneurons disrupts seizure initiation and maintenance
- The effects of inhibiting PV+ and SOM+ interneurons vary as seizures evolve

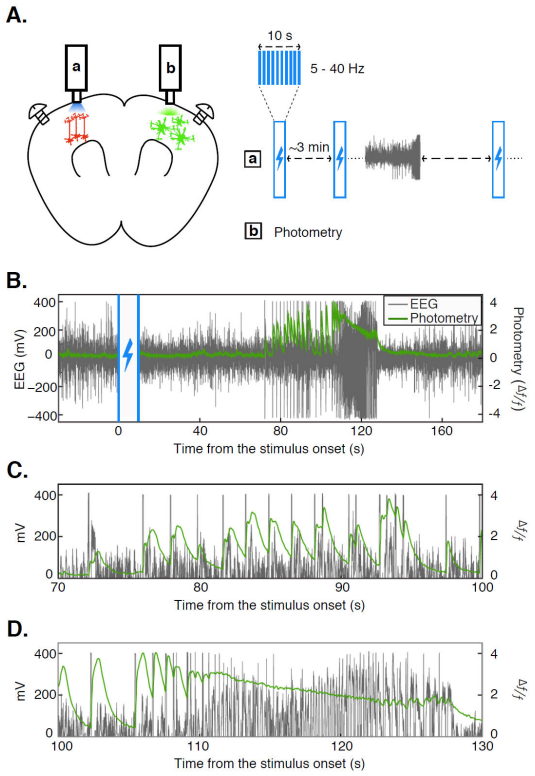

FIGURE 1. Simultaneous EEG recording and bulk calcium imaging in a mouse model for optogenetically-inducible seizures

A: Schematic illustrating the experimental design for optogenetic seizure induction as well as simultaneous EEG recording and photometry. For seizure induction, blue light was delivered through cannula a. For photometry, bulk fluorescence from neurons expressing GCaMP6f was captured through cannula b. Bilateral EEG was recorded via skull screws.

B: Example of simultaneous EEG and photometry recordings during a seizure in a SOM-Cre mouse. Time 0 marks the onset of the stimulus immediately preceding the seizure.

C: Example of simultaneous EEG and photometry recordings from panel B, zoomed in to illustrate the high correlation between the electrographic seizure activity and photometry signals.

D: Example of simultaneous EEG and photometry recordings from panel B, zoomed in to illustrate the temporal limitation of photometry in discerning individual epileptiform discharges at high frequencies.

See also Figure S1.

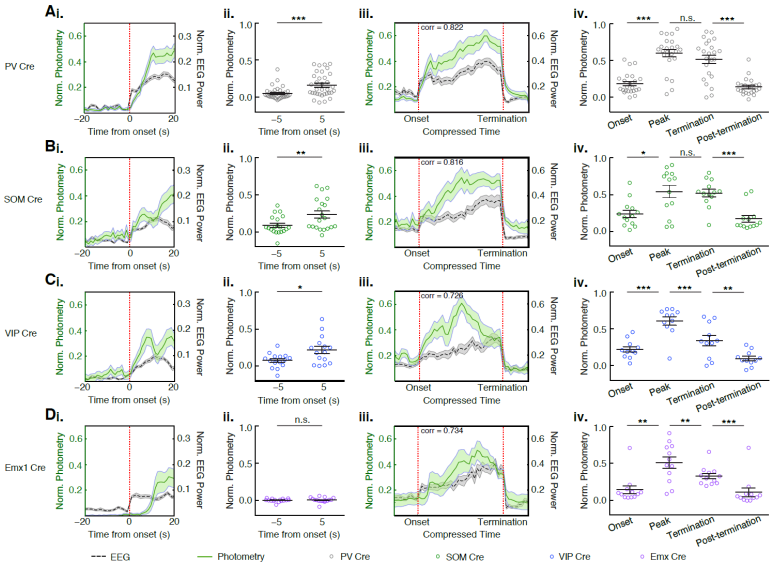

FIGURE 2. Interneurons and excitatory neurons exhibit distinct patterns of activity during seizures

A: (i) Mean EEG power—normalized to the peak EEG power during each seizure—and photometry signals—normalized to the peak photometry signal during each seizure—in PV Cre mice. Both recordings are aligned to the time of seizure onset (indicated by the dotted red line). **(ii)** Normalized photometry signals 5s before and after seizure onset. **(iii)** EEG power and photometry signals with compressed time, aligned to the time of seizure onset and seizure termination. Seizure onset and termination are indicated by the dotted red lines. **(iv)** Scatterplots showing photometry signals from individual seizures immediately after seizure onset (onset), at the peak —the same data point for all seizures— of the mean photometry trace (peak), one data point prior to seizure termination (termination), and 1s after seizure termination (post-termination).

B: Same as A, but for SOM-Cre mice.

C: Same as A, but for VIP-Cre mice.

D: Same as A, but for Emx1-Cre mice.

All data show means ± SEM and are analyzed using the two-tailed paired-sample t-test. Shading in the traces are ± SEM. Not significant (n.s.), $p<0.05$ (*), $p<0.01$ (**), $p<0.001$ (***). See also Figures S2 and S3.

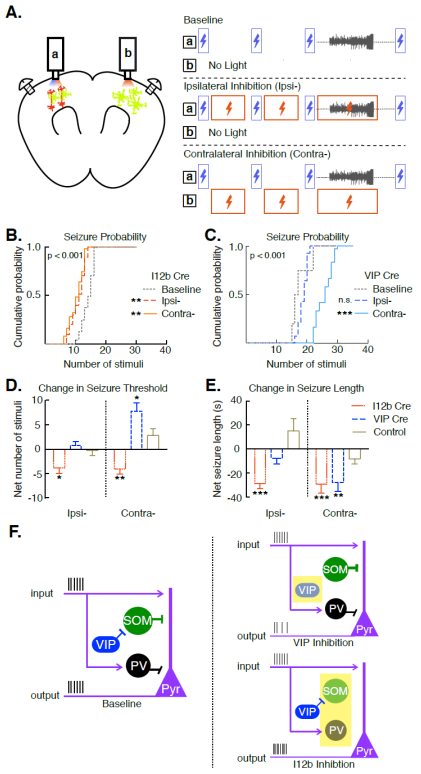

FIGURE 3. Cell type-specific optogenetic inhibition reveals different roles for DlxI12b+ and VIP + interneurons in seizure initiation and maintenance

A: Schematic illustrating the design of experiments using optogenetic inhibition of interneurons. For seizure induction, 445nm light was delivered through cannula a using the same protocol shown in Figure 1. Interneuron inhibition was achieved by delivering a constant 594nm amber light through cannula a or b. Experiments were performed on three consecutive days using three different conditions, as shown. Bilateral EEG was recorded via skull screws.

B–C: Cumulative probability for seizure induction as a function of the number of optogenetic stimuli delivered, in DlxI12b-Cre (B) and VIP-Cre (C) mice. “ipsi” and “contra” refer to inhibition of ipsilateral or contralateral interneurons, respectively, as shown in A.

D: Change in the number of stimuli required to induce the first seizure (seizure threshold) relative to baseline.

E: Change in seizure duration relative to baseline.

F: Schematic illustrating a simplified model for cortical microcircuits comprising interneurons and excitatory neurons during the pre-ictal stage. Arrows and flat lines symbolize excitatory and inhibitory synapses, respectively. Yellow boxes illustrate optogenetic inhibition.

All data show means ± SEM. Data in panels B and C are analyzed using one-way ANOVA and multiple comparisons test and data in panels D and E are analyzed using two-tailed student's t-test. In panels D and E, unless marked on the figure, there are no significant changes. Not significant (n.s.), $p<0.05$ (*), $p<0.01$ (**), $p<0.001$ (***).

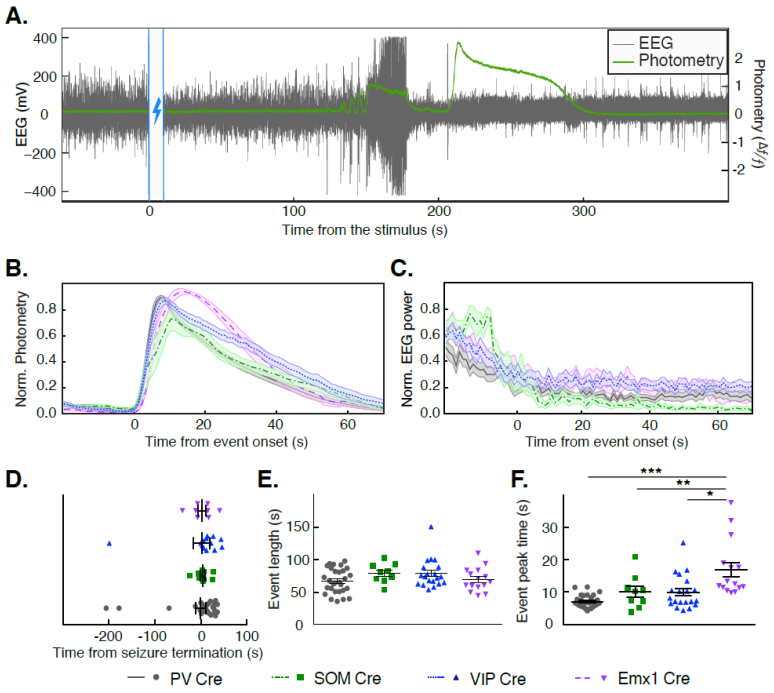

FIGURE 4. Cortical spreading depression (CSD)-like events associated with seizures

A: Example of simultaneous EEG and photometry recordings in a PV-Cre mouse demonstrating a CSD-like event during the post-ictal period. Time 0 marks the onset of the stimulus immediately preceding the seizure.

B: Mean photometry recordings—normalized to the peak of each CSD-like event—aligned to the onset of the CSD-like events.

C: Mean EEG power aligned to the onset of the CSD-like events.

D: Time of onset of each CSD-like event, relative to the time of termination of each seizure. Each data point is derived from a single seizure.

E: Duration of CSD-like events. Each data point is derived from a single seizure.

F: Time from the onset to the peak of each CSD-like event. Each data point is derived from a single seizure.

All data show means ± SEM and are analyzed using one-way ANOVA and multiple comparisons test. Shading in the traces and error bars in the scatter plots are ± SEM. In panels D through G, unless marked on the figure, there are no significant differences between different genotypes. $p<0.01$ (**), $p<0.001$ (***). See also Figure S4.